Çukurova Üniversitesi Mühendislik Mimarlık Fakültesi Dergisi, 28(2), 77-85 ss., Aralık 2013
Çukurova University Journal of the Faculty of Engineering and Architecture, 28(2), pp. 77-85, December 2013

Vortex Control of Cylinder Wake by Permeable Cylinder

Bengi GÖZMEN [*1], Hüseyin AKILLI[2], Beşir ŞAHİN[2]

[1]Faculty of Engineering, Department of Mechanical Engineering,Uşak University,Uşak,
[2] Faculty of Engineering & Architecture, Department of Mechanical Engineering, Cukurova University, Adana,

Abstract

In this present work, the flow control downstream of a circular cylinder in deep water using an outer permeable cylinder is studied experimentally. To reveal the effect of the porosity, eight different porosity values were selected as β=0,4, 0,5, 0,6, 0,65, 0,7, 0,75, 0,8 and 0,85. The ratio of outer cylinder diameter to inner cylinder diameter, D/d was selected as 2,5, i.e. the inner cylinder diameter is d=30 mm where the outer cylinder diameter is D=75 mm. The results indicated that the porosity is an important parameter to control the flow behind the inner cylinder - outer permeable cylinder arrangement. The outer permeable cylinder significantly suppresses the vortex shedding downstream of the inner cylinder-outer permeable cylinder arrangement with increasing the porosity until the porosities of β>0,75. The porosity of β=0,7 is the most suitable case to control the vortex shedding downstream of the circular cylinder.

Keywords: Passive control, PIV, Circular cylinder, Deep water.

Silindir Ardındaki Girdabin Ağ Yapılı Silindir ile Kontrolü

Özet

Bu çalışmada derin su içerisindeki dairesel silindir arkasındaki akışın silindir çevresine yerleştirilmiş ağ yapılı dış silindirler kullanarak kontrolüne çalışılmıştır. Geçirgenlik oranının etkisini anlayabilmek için sekiz farklı geçirgenlik oranı (β=0,4, 0,5, 0,6, 0,65, 0,7, 0,75, 0,8 ve 0,85) kullanılmıştır. Deneyler boyunca dış silindir çapının iç silindir çapına oranı D/d=2,5 olarak seçilmiştir. İç silindir çapı 30 mm iken, ağ yapılı dış silindir çapı D=75 olarak alınmıştır. Deneysel sonuçlar geçirgenlik oranının, silindir arkasındaki akışın kontrolü üzerine önemli etkileri olan önemli bir parametre olduğunu göstermektedir. Geçirgenlik oranı 0,75'e kadar geçirgenlik oranın artmasıyla, ağ yapılı dış silindir dairesel silindir arkasındaki girdap dökülmesini önemli derecede azaltır. Geçirgenlik oranı β=0,7 değeri, akış kontrolünün en iyi sağlandığı durumdur.

Anahtar Kelimeler: Pasif kontrol, PIV, Dairesel silindir, Derin su.

[*] Yazışmaların yapılacağı yazar: Bengi GÖZMEN, *Faculty of Engineering, Department of Mechanical Engineering,Uşak University Uşak, bengigozmen@gmail.com*

1. INTRODUCTION

The vortex shedding downstream of bluff bodies causes negative effects on a large number of engineering applications. The vortex shedding which may cause structural vibrations and acoustic noises, and shorten the life of the bluff body is accompanied by a large fluctuation of drag and lift forces. Because of these negative effects, methods of suppression of vortex shedding from bluff bodies have been widely investigated both numerically and experimentally. In order to prevent the problems due to the vortex shedding, two main flow control techniques are used: active and passive control. Active control methods are based on applying some sorts of external energy into the flow field while the passive control techniques control the vortex shedding by modifying the shape of the bluff body or by attaching additional devices in the flow. Splitter plates, small rods, base bleed, roughness elements, helical wires and porous and permeable structures are examples of passive control techniques.

Lee et al. [1] studied on the effects of a small control rod on drag characteristics and wake structure behind the cylinder. They placed a small control rod upstream of the cylinder. They reported that the drag coefficient and wake structure changed significantly depending on pitch distance L between the main cylinder and control rod. Wang et al. [2] investigated effect of a rod on the drag reduction around a circular cylinder. They observed that the existence of the control rod was effective on drag and lift reduction. The flow characteristics of the wakes behind circular cylinders fitted with o-rings were investigated by Lim and Lee [3]. They revealed that the vortex formation region behind the cylinder fitted with o-rings extended and drag force acting on the cylinder decreased at high Reynolds number. The thickness effects of splitter plate on the vortex shedding downstream of a circular cylinder was studied experimentally by Akilli et.al. [4]. They showed that the change in the thickness of splitter plate did not have any considerable effect on the flow structure. And the splitter plate had influence on the suppression of vortex shedding for the gap ratio between 0 and 1,75D. Yucel et al. [5] studied on the effect of a detached downstream plate on the near wake of a circular cylinder. The experiments were carried out for five different horizontal (G) and seven different vertical (Z) locations between the cylinder and the plate. They observed variations in vortex shedding as a function of vertical and horizontal distances between the body and the plate. Gozmen et al. [6] investigated the effects of splitter plates having different heights and lengths located in the wake region of the circular cylinder in shallow water. They obtained that flow structures changed significantly with height and length ratios of the splitter plates in shallow water. The wake region downstream of the cylinder elongated along the streamwise direction with increasing plate length and depth. The case of h_p/h_w=0,75 for L/D=2 was the most effective case on the control of vortex shedding.

Porous and permeable devices are other devices in order to control the flow around bluff bodies. Sobera et al. [7] investigated flow structure at subcritical Reynolds number (Re=3900) around a circular cylinder surrounded by porous layer. They found that the flow in the space between the porous layer and the solid cylinder was laminar and periodic and the frequency of flow was locked to the Strouhal frequency of vortex shedding in wake region. Bhattacharrya et al. [8] studied on flow structure around and through a porous cylinder. They revealed that the flow field was steady for the range of Reynolds number ($1 \leq Re \leq 40$) and the drag experienced by the porous cylinder decreased monotonically while the Reynolds number was increasing and the Da was decreasing. Kleissl and Georgakis [9] researched the effects of bridge cable shape and surface on the control of wind-induced vibrations. They used four different cable shapes a circular cylinder, ashrouded cylinder, a wavy and a facetted cylinder to compare with each other. They revealed that the effect of shrouded cylinder on the flow depends on Reynolds number slightly. And the shrouded cylinder significantly reduced the vortex-induced oscillating lift forces. The drag coefficient was measure as slightly above 1,0. Flow structure around a cylinder surrounded by a permeable cylinder in shallow water was investigated

experimentally by Ozkan et al. [10]. This study observed that both porosity and outer cylinder diameters had significant effects on control of wake region downstream of the circular cylinder in shallow water. The peak values of turbulent statistics like turbulent kinetic energy, Reynolds stresses were diminished considerably by the outer permeable cylinder.

The main aim of present investigation is to reveal the effect of permeable cylinder placed around a circular cylinder with a diameter of 30 mm in deep water. The effect of porosity β on the vortex control downstream of the circular cylinder has been focused on. So, eight different porosities were used in order to prevent the harmful effects of vortex shedding on many engineering applications where the permeable cylinder would be used as a control device such as bridge piers and risers in off-shore engineering etc.

2. MATERIAL and METHOD

Experiments were performed by using Particle Image Velocimetry technique in a circulating open water channel having dimensions of 8000 mm x 1000 mm x 750 mm located at Fluid Mechanics Laboratory of Mechanical Engineering Department of Cukurova University.

In this study, the effects of the porosity are investigated. Porosity is defined as the ratio of the gap area on the body to the whole body surface area. Porosity value is calculated by using the following formula including wire diameter and distance between two wires (x). It is shown in Figure 1.

Permeable cylinders were constructed from chrome-nickel wire mesh. And eight different wire meshes were used corresponding to eight values of porosity as β = 0,4, 0,5, 0,6, 0,65, 0,70, 0,75, 0,80 and 0,85. A permeable outer cylinder having the diameter of D=75 mm was concentrically located around the inner cylinder with the diameter of d=30 mm in order to suppress the vortex shedding downstream of the inner cylinder. The placement of inner cylinder-outer permeable cylinder arrangement is presented in Figure 2.

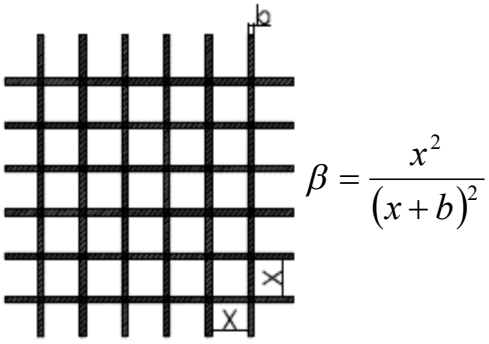

Figure 1. Calculation of the porosity, β

During the all experiments, the free stream velocity was U = 0,156 m/s, which corresponded to Reynolds number of Re_i = 5000 based on the inner cylinder. All experiments were carried out above a platform and the height of the water (h_w) was adjusted to a 340 mm height as all experiments. The laser sheet was located parallel to the bottom of the water channel at a height of h_L/h_W= 0,45 for all cases.

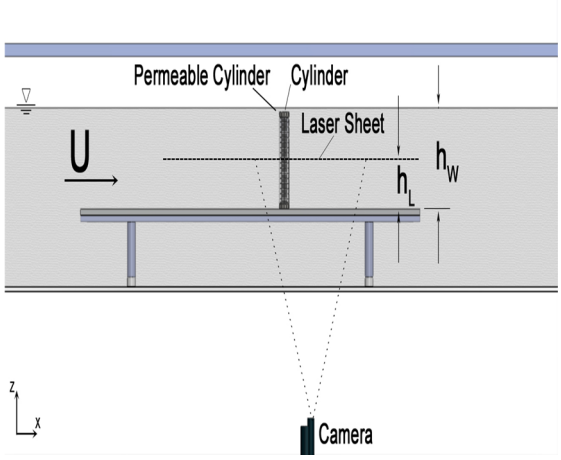

Figure 2. Side view of the experimental setup

The PIV technique is employed to calculate instantaneous and mean velocity field behind a circular cylinder in order to understand the effect of the permeable cylinders on the vortex shedding behavior in deep water. The experimental data was acquired and processed using Dantec Dynamics

PIV system and Flow Manager software installed on a computer. The measurement field was illuminated by a thin and an intense laser light sheet by using a pair of double-pulsed Nd:YAG laser units each having a maximum energy output of 120 mJ at 532 nm wavelength. The thickness of laser sheet was adjusted approximately to 1,5 mm. The laser sheet was oriented parallel to the bottom surface of the water channel and the laser light sheet was at the height of 155 mm from the platform. The water was seeded with 12μm, metallic-coated hollow plastic spheres. The movement of particles was recorded by a CCD camera with a resolution of 1024x1024 pixels. The camera was equipped with a Nikon AF Micro 60 f/2,8 D lens. In the image processing, 32×32 rectangular interrogation pixels were used and an overlap of 50% was employed. A total of 3844 (62×62) velocity vectors were obtained for an instantaneous velocity field at a rate of 15 frames/s. Spurious velocity vectors (less than 2%) were omitted using the local median-filter technique and replaced by using a bilinear least squares fit technique between surrounding vectors. The vorticity value at each grid point was computed from the circulation around the eight neighboring points. In each experiment, 350 instantaneous images were captured and recorded in order to have the time-averaged velocity vectors and flow field of other statistical properties. During the flow measurement, two flow fields were taken because a single field of view was inadequate to gain the flow characteristics of the wake region. Each field of view was 200x200 mm^2.

3. RESULTS and DISCUSSION

By this study, control of the unsteady flow structure behind a circular cylinder having D_i=30 mm diameter in deep water was intended. At first, flow characteristics of bare (inner) cylinder are investigated to compare with the inner cylinder-permeable outer cylinder arrangements. To explain the flow structure, normalized Reynolds stress contours, dimensionless turbulent kinetic energy contours and the streamwise velocity contours are shown in Figure 3. The normalized Reynolds shear stress contours $< u'v' >$ is indicated in the first row. The minimum and incremental values of Reynolds shear stress were selected as ± 0,002 and 0,002, respectively. While the solid lines present the positive (counter-clockwise) Reynolds shear stresses, the dashed lines show the negative (clockwise) Reynolds shear stresses as the all figures in this study. It is understood that both the positive and negative Reynolds shear stress contours $< u'v' >$ elongate symmetrically along the centerline of the cylinder. The well-defined Reynolds stresses due to the fluctuations in the shear layers produce a weaker Reynolds stress region very close to the base of the cylinder which occurs as a consequence of the flow entrainment into the wake region. The peak value of Reynolds shear stress $< u'v' >$ is approximately 0,0405. In the second row of Figure 3, the turbulent kinetic energy (TKE) contours are represented. For the

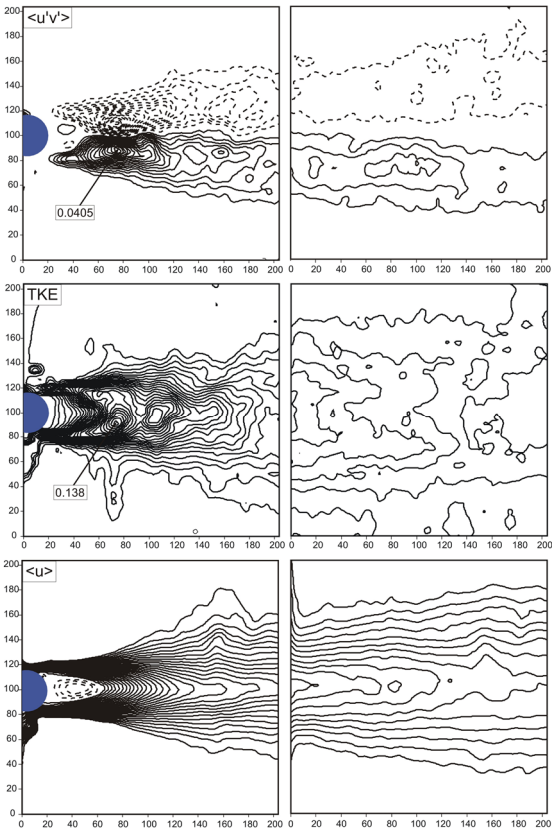

Figure 3. Results obtained from PIV for the bare cylinder

contours of TKE, both minimum and incremental values were taken as 0,005. The peak value of turbulent kinetic energy is 0,138 in the first field of view. The location of peak value of TKE coincides with the location of peak value of the Reynolds shear stress. After the location of the peak value, the turbulent kinetic energy starts to dissipate gradually in the flow direction. The last row indicates the contours of time-averaged streamwise velocity $< u >$. The minimum and incremental values of the streamwise velocity contours were selected as ± 5 and 5, respectively. The substantial region of reverse flow is evident at the bare cylinder case as a result of momentum transfer from the free-stream flow into the wake region. The location of negative velocity contours is approximately 1d from the base of the cylinder and the peak value of negative streamwise velocity is nearly 0,121.

In order to reveal the effect of the porosity on the flow control downstream of the inner cylinder-outer permeable cylinder arrangement for the diameter ratio of D/d= 2,5, the contours of normalized Reynolds shear stress $< u'v' >$, turbulent kinetic energy (TKE) and the time averaged streamwise velocity component $< u >$ are shown in this study. The concentrations of Reynolds shear stress are indicated in Figure 4. The minimum and incremental values of Reynolds shear stress were selected as ± 0,002 and 0,002, respectively. For the porosity values of β = 0,4 and 0,5, the wake region downstream of the inner-outer cylinder arrangement elongates along the streamwise direction. However, the maximum Reynolds shear stress concentrations do not decrease considerably. In the range of 0,6≤β≤0,7, the positive efficiency of outer permeable cylinder with the diameter of 75 mm increasingly continues. The concentration of Reynolds shear stress weakens with increasing the porosity values from 0,6 to 0,7. This decrease in the Reynolds shear stress may be directly related to the drag force reduction of the inner cylinder as obtained by Fujisawa and Takeda [11], Kim et al. [12]. Additionally, as the peak values of Reynolds shear stress of porosities less than 0,75 locate in the second field of view, the peak values of $< u'v' >$ occur just behind the outer permeable cylinder in the first field of view for β ≥ 0,75 and the peak values of Reynolds shear stress drop to 0,0145, 0,0176 and 0,0196 which are a bit greater than that of the porosity of β = 0,7, respectively. Furthermore, the Reynolds shear stresses cover the wake region of the inner-outer cylinder arrangement for the range of 0,75 ≤ β ≤ 0,85 as a result of increasing effect of the inner cylinder on the flow structure.

In terms of TKE, the peak value of TKE decreases significantly in comparison to the bare cylinder case for all porosities as can be seen in Figure 5. The presence of the outer permeable cylinder strongly attenuates the large scale vortices which carry fresh fluid from the free-stream region into the wake region and then velocity fluctuations downstream of the inner-outer cylinder arrangement are weakened. In the range of 0,4 ≤β ≤ 0,75, the peak value of TKE is suppressed by the outer permeable cylinder as the porosity value rises. The maximum reduction in turbulent kinetic energy is obtained from the case of β = 0,75.

Moreover, for the range of 0,4≤β≤0,7, the location of peak value of TKE moves further away from the base of the inner-outer cylinder arrangement except the porosity of β = 0,5 as a sign of effective control of vortex shedding in the wake region. For porosities of β = 0,8 and 0,85, the unsteady vortices, which take place in the annular region between the inner cylinder and the outer cylinder, cause an increase in the turbulent kinetic energy just downstream of the outer cylinder. Moreover, two peaks of TKE for the porosity values of β=0,8 and 0,85 are obtained in the wake region on account of the unsteady vortices mentioned above.

Figure 6 shows the contours of the time averaged streamwise velocity $< u >$ for all porosities. The minimum and incremental values of the streamwise velocity component were adjusted as ± 5 and 5, respectively. When the contours of streamwise velocity $< u >$ are investigated, it is understood that the outer permeable cylinder

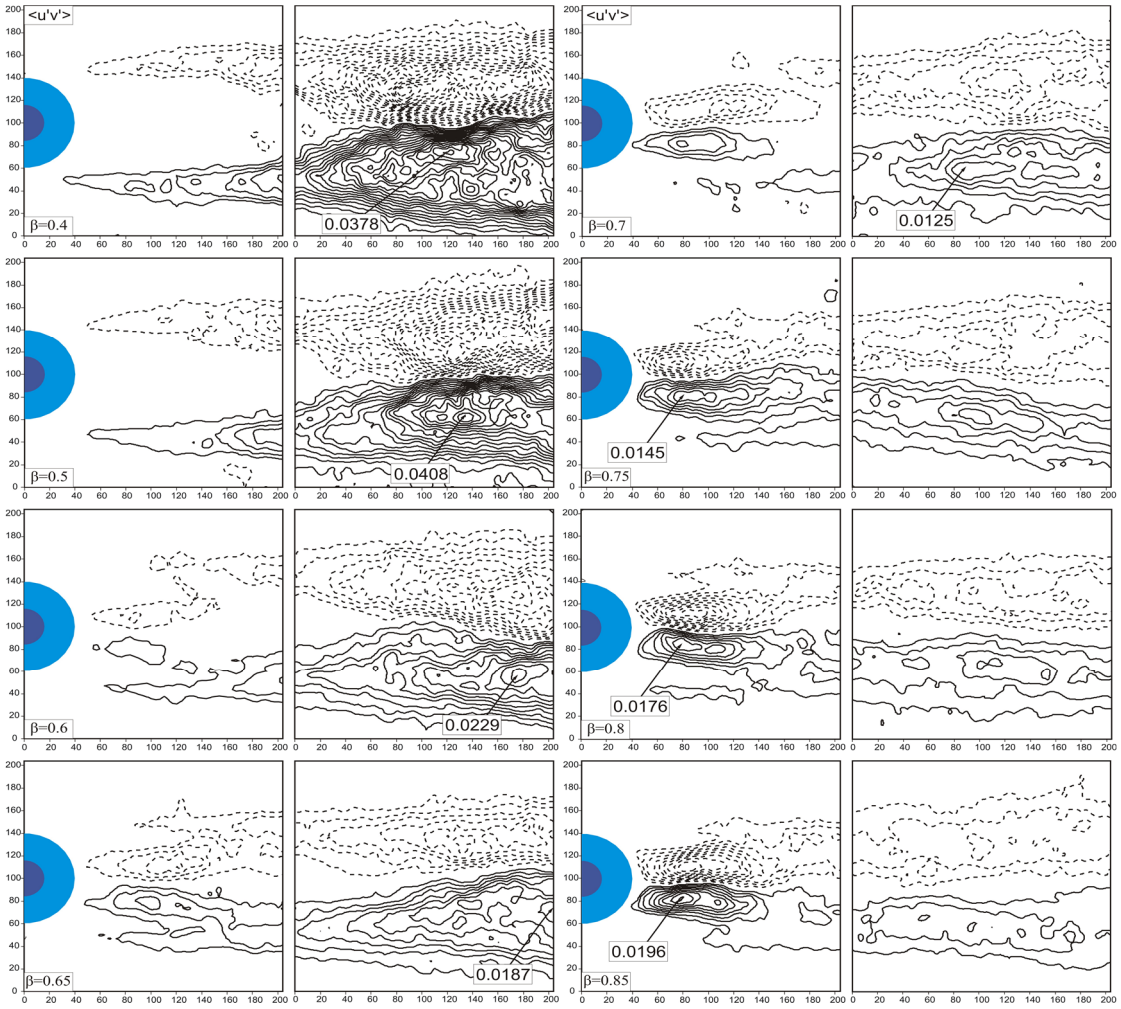

Figure 4. Contours of normalized Reynolds shear stress downstream of the inner cylinder-outer permeable cylinder arrangement for the diameter ratio of D/d = 2,5

prevents the forming of reverse flow for the porosity range of $0,5 \leq \beta \leq 0,7$. For these cases, the momentum transfer from the free-stream region into the wake region is prevented. On the other hand, for the porosity of $\beta = 0,4$, occurance of the reverse flow is obviously seen due to the fact that the permeable cylinder having the porosity of $\beta = 0,4$ behaves like a solid cylinder. Fortunately, the reverse flow in the wake region for the porosity of $\beta = 0,4$ forms in the second field of view and the reduction in the negative streamwise velocity is approximately 32 % of that of the bare cylinder. For the cases of $\beta = 0,8$ and 0,85, the reverse flow exists in the base of the outer cylinder and the magnitude of negative streamwise velocity is less than that of the bare cylinder case. For these cases, the flow penetrates from the open area on the surface of the outer permeable cylinder into the wake region and the unsteady flow structure occured by the inner cylinder is more effective than that of the outer permeable cylinder. Another meaning of this flow structure is that the

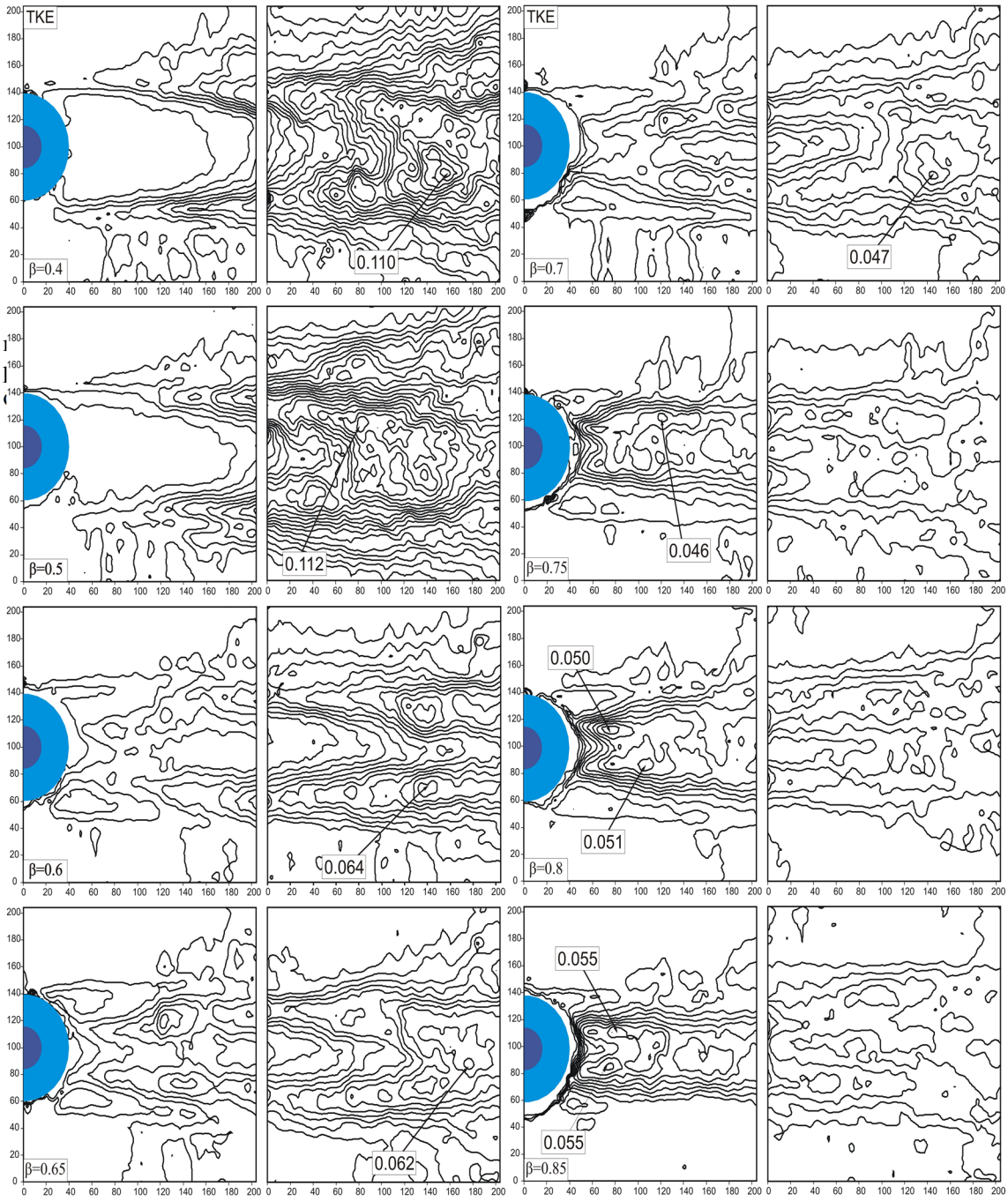

Figure 5. Contours of turbulent kinetic energy downstream of the inner cylinder-outer permeable cylinder arrangement for all porosity values β of the diameter ratio of D/d = 2,5. The minimum and incremental values of TKE were taken as 0,005

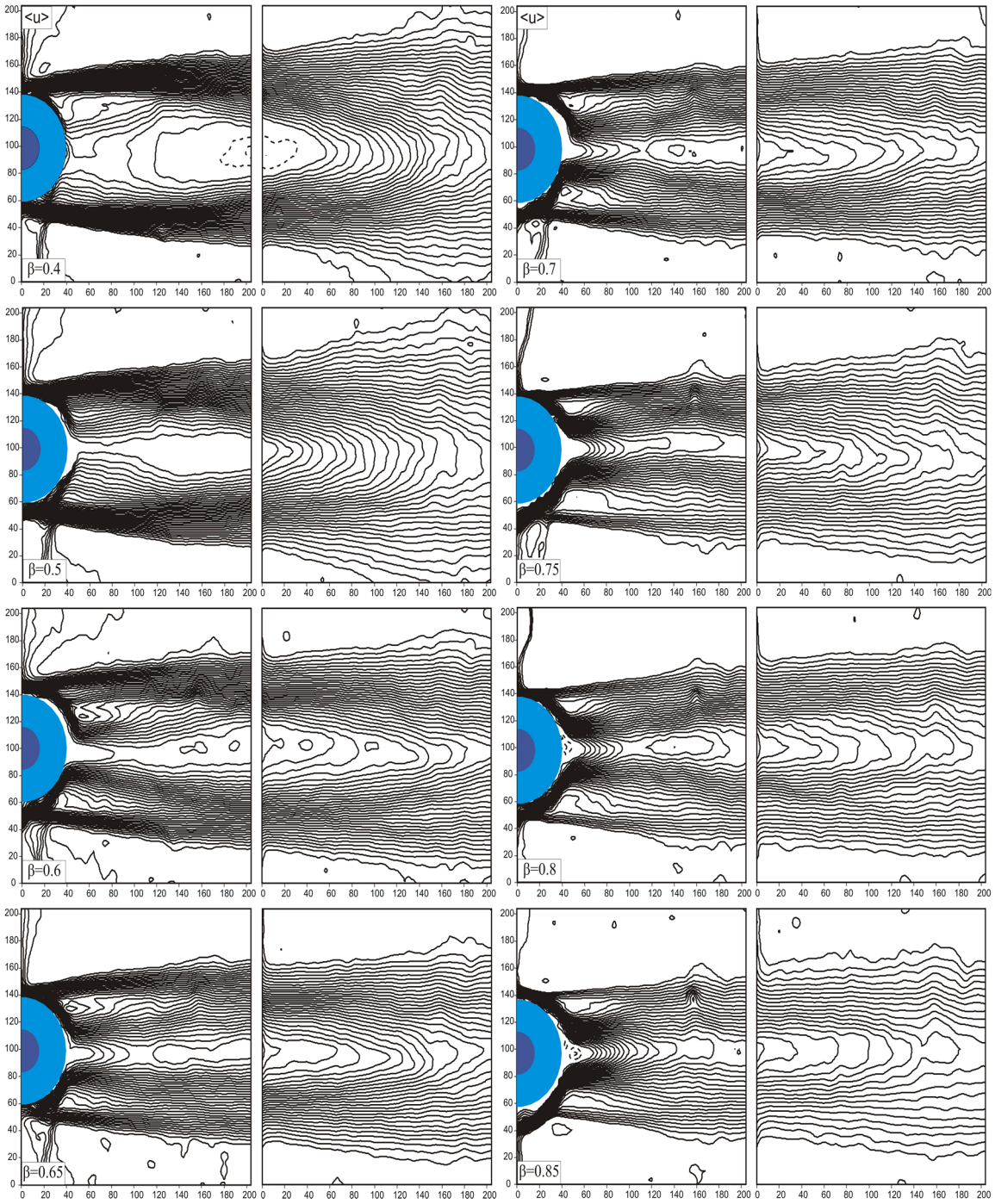

Figure 6. Contours of time-averaged streamwise velocity downstream of the inner cylinder-outer permeable cylinder arrangement for all porosity values β of the diameter ratio of D/d =2,5

momentum transfer is provided by the flow passage from the open area on the surface of the outer permeable cylinder into the wake region.

4. CONCLUSIONS

The purpose of this study is to control the flow downstream of a circular cylinder in deep water using a surrounding outer permeable cylinder. The results obtained in this study demonstrate that the unsteady flow downstream of the cylinder is controlled and turbulent intensity is reduced considerably for all porosities in the first view field. The porosity of β=0,7 is the most suitable case to control the flow downstream of the circular cylinder. For this porosity, the occurrence of Von Karman Vortex Street is not seen. The momentum transfer from the free stream flow into the wake region is prevented. Furthermore, the turbulent intensity of the flow is reduced at most 70% by the presence of outer permeable cylinder compared to the bare cylinder case. For remaining porosity values, the permeable cylinder is still effective on control the flow, but the efficiency of these porosity values is less than that of the porosity of β = 0,7.

5. REFERENCES

1. Lee, S.J., Lee, S.I., Park, C.W., 2004. Reducing The Drag on a Circular Cylinder by Upstream Installation of a Small Control Rod. Fluid Dynamics Research, 34:233-250.

2. Wang, J.J., Zhang, P.F., Lu, S.F., Wu, K., 2006. Drag Reduction of a Circular Cylinder Using an Upstream Rod. Flow Turbul Combust, 76:83–101.

3. Hee- Chang, L., Sang- Joon, L., 2004. Flow Control of a Circular Cylinder with O-Rings. Fluid Dynamics Research, 35:107-122.

4. Akıllı, H., Sahin, B., Tumen, N.F., 2005. Suppression of Vortex Shedding of Circular Cylinder in Shallow Water by a Splitter Plate. Flow Meas Instrum, 16:211–219.

5. Yücel S.B., Çetiner O., Unal M.F., 2010. Interaction of Circular Cylinder Wake with a Short Asymmetrically Located Downstream Plate. Exp Fluids 49: 241-255.

6. Gözmen, B., Akıllı, H., Şahin, B., 2013. Passive Control of Circular Cylinder Wake in Shallow Flow. Measurement 46:1125-1136.

7. Sobera, M.P., Kleıjn, C.R., Van Den Akker, H.E.A., 2006. Subcritical Flow Past A Circular Cylinder Surrounded by a Porous Layer, Phys. Fluids 18: 038106.

8. Bhattacharyya, S., Dhınakaran, S., Khalili, A., 2006. Fluid Motion Around and Through A Porous Cylinder. Chemical Engineering Science, 61:4451-4461.

9. Kleissl, K., Georgakis, C.T., 2011. Aerodynamic Control of Bridge Cables Through Shape Modification: A preliminary Study, Journal of Fluids and Structures 27:1006–1020.

10. Ozkan, M.G., Oruç, V., Akıllı, H., Şahin, B., 2012. Flow Around a Cylinder Surrounded by a Permeable Cylinder in Shallow Water. Exp Fluids, 53:1751–1763

11. Fujısawa, N., Takeda, G., 2003. Flow Control Around a Circular Cylinder by Internal Acoustic Excitation. J Fluid Struct, 17: 903–913.

12. Kim, W., Yoo, J.Y., Sung, J., 2006. Dynamics of Vortex Lock-On in a Perturbed Cylinder Wake. Phys Fluids, 18: 074103.